

Study of URT-1M accelerator in submicrosecond operation

M.E. Balezin^{1,}, S.Yu. Sokovnin^{1,2}, A.S. Gerasimov^{1,2}*

¹*Institute of Electrophysics UB RAS, Yekaterinburg, Russia*

²*Ural Federal University named after First President of Russia B.N. Yeltsin, Yekaterinburg, Russia*

**mk@iep.uran.ru*

Abstract. The purpose of this work was to investigate the operation of the URT-1M accelerator with a power system without SOS switch. The approaches used in the high-voltage pulse generation system of this accelerator allow generating a pulse with an amplitude of up to 500 kV, a duration of ~450 ns and a supply repetition rate up to 50 pps during discharge of the second circuit capacitor. It was found that in this mode, an accelerator with a metal dielectric cathode works stably at a charging voltage of up to 35kV (accelerating ~350 kV). Further increase of voltage is limited by breakdown of feedthrough vacuum insulator with shielding of dielectric surface.

Keywords: radiation surface disinfection, electron accelerator, electron beam.

1. Introduction

In recent years, the concept of surface radiation sterilization (SRS) has been actively developing, the essence of which is the effect of an electron beam only on the surface layer of the irradiated object. This approach is promising in many applications, such as the processing of various food products (grains [1], eggs [2] and lump meat [3]), feed [4] or packaging [5]). The main advantage of the SRS is the ability to localize changes in the product in a narrow surface layer (tens to hundreds of microns), which is contaminated with various microorganisms. In this case, the main part of the product is irradiated only by bremsstrahlung, the level of absorbed doses in which is tens of thousands less than on the surface. This allows to maintain not only the nutritional value of the main part of the product, but also the vitality of seeds or eggs.

At the same time, the requirements for maximum electron energy for such accelerators are significantly reduced to 0.5–1 MeV, and the presence of low-energy electrons in the spectrum becomes useful. These electrons enhance the irradiation of surface layers and reduce the output of inhibitory radiation, the only limitation is to become their high absorption in the output foil, and increases the thermal load on it.

Currently, several approaches are used to create accelerators in this energy range. For all its advantages, ELV accelerators [6] have excessive power and high cost, which limits their use. An interesting approach was used in the creation of accelerators of the Scan type [5], which makes them very competitive. A high-current accelerator TEMP [7] has certain advantages, the main drawback of which is due to the presence of a spark gas switch in the high-voltage pulse generation circuit. This drawback was eliminated in the high-current ASTRA-M accelerator [8], but the high-current mode of operation complicates the operating conditions of the cathode and does not allow obtaining a long lifetime ($>10^6$ pulses).

Accelerators such as URT [9] are used for various applications: including for SRS [10]. The main disadvantage of such accelerators is that the generation circuit contains an SOS switch, which on the one hand leads to an increase in the output voltage, but reduces the efficiency of transmitting energy to the electron beam due to the fact that the SOS switch is located parallel to the load.

An interesting solution is used when creating an accelerator (475 keV) with a pulse transformer [11] with a pulse duration at half-altitude of 0.25 μ s. For all the advantages of this accelerator, it is not devoid of disadvantages. First of all, this is a relatively large energy in the pulse (225–1125 kJ at a charging voltage of 75 kV) and the beam current (1.5 kA), which on the one hand limit the pulse repetition rate (5 pps), and on the other, as in other high-current accelerators, complicate the operating conditions and reduce the cathode life ($\sim 10^5$ pulses). An excessive dose per impulse can

also be noted, which complicates the adjustment for specific technologies. All this will complicate the commercial use of this accelerator for the SRS.

The purpose of this work was to conduct research on the creation of a submicron-duration electron accelerator based on the power supply system of the URT-1M accelerator [12]. The approaches used in the high-voltage pulse generation system of this accelerator make it possible to form a pulse with an amplitude of up to 500 kV, a duration of ~ 450 ns and a pulse repetition rate up to 50 pps when the capacitor C1 is discharged. At the same time, the main problems are whether the vacuum feedthrough insulator with shielding of the dielectric surface [13] is able to withstand such high-voltage pulses, and the metal-dielectric cathode [14] has the necessary emission capacity.

2. Experimental Installation Description and Experimental Procedures

To test the concept was used the URT-1M accelerator from the circuit of which [12] the SOS key was removed (Fig.1).

The pulse transformer (PT) is wound on a core of three rings K650 \times 470 \times 25 mm made of permalloy 50NP 20 μ m thick. Between the rings there is a gap of 3 mm for cooling. The transformation ratio is 10, the scattering inductance is 0.8 μ H. Windings are made of copper tape 0.5 mm thick: secondary tape 30 mm wide, and primary tape 50 mm. The primary winding overlaps about 1/3 of the secondary, which is wound on an acryl frame. Insulating gaps of core-winding and between windings are 25 mm. To effectively remagnetize the core of the pulse transformer, a recuperation circuit is used consisting of a VD1 diode (0.4/125 SDLK) and an inductor ($L_p = 20$ μ H, see Fig.1). The inductance of the additional solenoid $L_s = 6.4$ μ H.

Capacitance of the primary circuit capacitor is $C_0 = 84.1$ nF, structurally it is made in the form of 17 parallel sections of five KVI-3-12kV-6800pF capacitors connected in series. Capacitance of the secondary circuit capacitor is $C_1 = 650$ pF, structurally it consists of four parallel sections of 28 capacitors KVI-3-12kV-6800pF connected in series. Thyatron TGI1-2500/50 (V1) was used for switching.

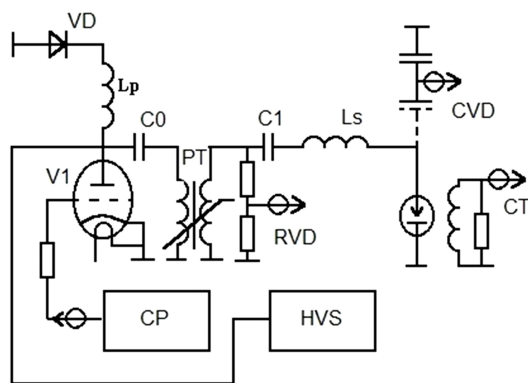


Fig.1. Diagram of experimental installation.

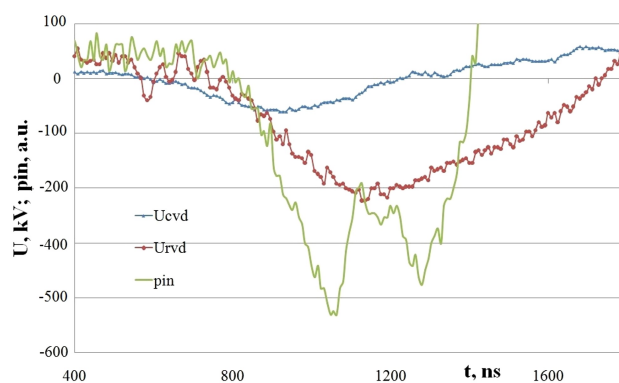


Fig.2. Oscillograms by $U_0 = 25$ kV.

The high voltage pulse generation circuit and vacuum diode are immersed in transformer oil and placed in a square metal housing (900 mm side) 1300 mm high with a water jacket at the top for cooling. The high voltage source (HVS) converts the 380V network voltage to an adjustable DC voltage of up to 50 kV. The accelerator is controlled remotely from the control panel (CP).

Vacuum diode of two side irradiation [15] with beam width up to 500 mm was pumped out by diffusion pump N-250. However, in experiments was used only the upper diode with a metal dielectric cathode with a diameter of 40 mm [14]. For beam output, the vacuum diode has an outlet window with a width of 50 \times 500 mm. It has an aluminum grid with 85% transparency, consisting of

slots and ribs 10 mm and 2 mm wide, respectively. An output aluminum foil with a thickness of 30 μm is laid on the grid.

Feedthrough vacuum insulator (FVI) is made with shielding of dielectric surface [13]. It consists of three acryl rings of 120 mm high. The outer and inner diameters of the rings are 394 and 220 mm, respectively, the angle of inclination of the inner polished (Ra 6.3) surface is 60° . Distance of sliding of screen end relative to high-voltage edge of insulator was along radius 9 mm, and along length 40 mm, respectively. During the experiments, the sections of the insulator were bridged on the oil side with metal shortcuts.

The voltage at the forming capacitor $C1$ and the voltage at the vacuum diode were measured using resistive (RVD) and capacitive (CVD) voltage dividers, respectively. The electron beam current at the output of the vacuum diode was measured using a current transformer (CT) in the anode flange. Electrical pulses were recorded on the Tektronix TDS 3014B digital oscilloscope.

The dosimetric method [16] was used to control electrical measurements. To measure the dose rate of bremsstrahlung was used a semiconductor detector SKD1-02 with a block of separating capacitors SBR-21, which was installed at a distance of 170 mm. The absorbed dose of the electron beam was measured by a plastic detector of the type SD PD (F) R-5/50, part of which was covered with an absorber of different number of layers of aluminum foil with a thickness of 20 μm , to measure the electron energy by the gray wedge method.

3. Results of experiments and their discussion

Experiments were performed at a charging voltage of HVS U_0 from 20 to 40 kV. Oscillograms at $U_0 = 20$ kV showed that the time constants of the sensors: CT, pin-diode and CVD are not enough. This results in the signals from these sensors being informative only at the front of the pulse. It was found that the beam current is formed practically without delay, and the vacuum gap of the cathode-anode (125 mm) does not overlap during the action of the accelerating voltage (~ 1 μs). Voltage pulse rise time $t_1 \sim 450$ ns and decay time $t_2 \sim 850$ ns, respectively (Table 1). The impedance of the vacuum diode calculated from the decay time constant is $R_d \sim 3$ kOhm, which roughly corresponds to the current amplitude. Bridging of the one or two sections of the vacuum insulator does not affect the shape of the accelerating voltage and the amplitude of the first peak of the pin-diode.

Table 1. Results of experiments

U_0 , kV	t_1 , ns	t_2 , ns	R_d , kOhm	pin-diode
20	450	850	3	314
25	480	720	2.4	862
30	464	440	1.49	1410
35	480	288	975	912
40	352	123	325	143

With an increase in $U_0 = 25$ kV (Fig.2), the amplitude of the pin-diode signal increased by 2.7 times (Table 1). This increase in the amplitude of the dose rate of bremsstrahlung is well described by the Forster formula [16], while partially increasing due to an increase in voltage (to the extent of $(250/200) 2.8 = 1.8$) and due to a decrease in impedance by 1.5 times. In addition, this indicates the correctness of using the first peak of the pin-diode signal in relative units. Bridging of 1 or 2 sections of the vacuum insulator does not affect the shape of the accelerating voltage (Fig.3) and the amplitude of the first peak of the pin-diode.

With a further increase in U_0 to 30 kV is observed a similar picture (Table 1), however, breakdowns began on the vacuum side of the complete insulator, which were well diagnosed on both types of dividers and on the pin-diode signal (Fig.4) too. The bridging of the 1st or 2nd

sections made it possible to establish that the breakdowns are connected to one of the sections of the insulator and occur not over the entire surface of the dielectric (Fig.5), but at one point of the surface of the insulator closest to the end of the screen on the end itself.

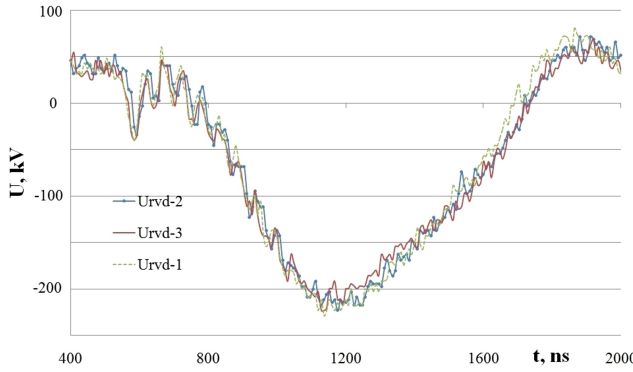


Fig.3. Oscillograms ($U_0 = 25$ kV) by different number of sections of FVI.

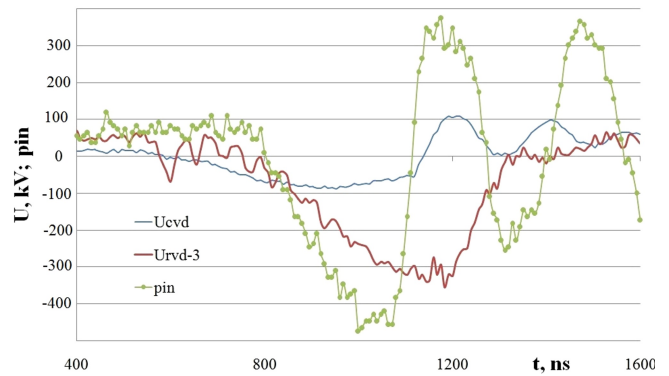


Fig.4. Oscillograms by $U_0 = 30$ kV for full insulator.

The breakdowns were the result of misalignment of manufacture, as well as the presence of a processed weld on the screen at this place. It should be noted that in the mode of the accelerator operation according to the standard electrical scheme with an SOS switch at a voltage up to 1MV and a pulse repetition rate up to 50 pps, insulator breakdowns were not observed, even during the long-term operation of the accelerator (6 hours). The closure of the defective section of the insulator led to the restoration of the accelerator operation, both at 2 and 1 section (Fig.5).

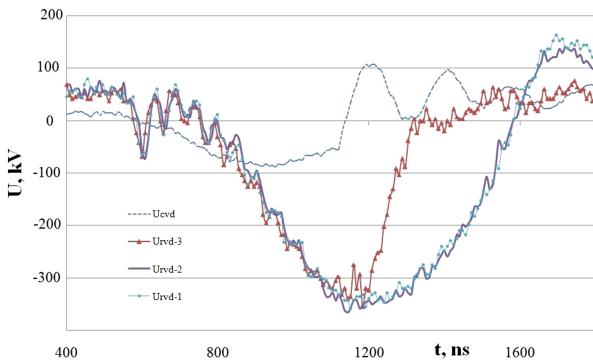


Fig.5. Oscillograms ($U_0 = 30$ kV) by different number of sections of FVI.

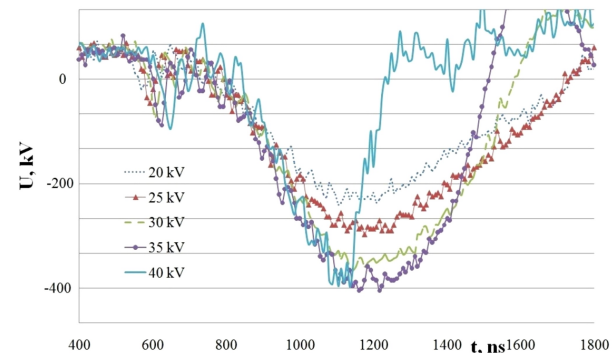


Fig. 6. Oscillograms by different U_0 for 2 section of FVI.

A further increase in U_0 to 40 kV made it possible to establish that the greatest electrical strength is achieved with two operating sections of the insulator, but the operation of the insulator at $U_0 = 40$ kV is short-term, after which breakdowns begin (Fig.6). It should be noted that the increase in electrical strength at two operating sections of the insulator is not significant compared to one that operates at $U_0 = 35$ kV.

Thus, it can be stated that in the submicrosecond region of time, the Martin formula does not work for FVI with dielectric surface shielding, although it worked perfectly in the region of times 20–60 ns [13]. As can be seen from the data of Table 1, the impedance of the vacuum diode drops at a $U_0 \geq$ of 35 kV without increasing the pin-diode signal. This suggests the ignition of a parallel discharge or emission from the cathode holder to the grounded screen of the PVI, as observed in [17].

Comparison of different types of insulators was performed in operation [17] at voltage pulses with duration at FWHM ~ 400 ns (10 ns front), which showed that FVI with dielectric surface shielding (4 polyethylene rings of 110 mm each with an angle of 60° , with an inner diameter of the insulator of 234 mm) transmits such a pulse for ~ 100 ns and ~ 300 ns at a voltage of 800 kV and 900 kV, respectively. A solution to the problem was found by lengthening all the shields for the full length of the insulator, which provided an average strength along the dielectric surface of ~ 40 kV/cm, possibly due to a magnetic mole of flowing current (20 kA).

In our case, the voltage pulse had a different shape (a FWHM ~ 450 ns with a relatively small current), so it was hoped to obtain a high electrical strength of the insulator by reducing the time $t_{0.89}$, which did not materialize. It should be noted that after stopping the supply of high-voltage pulses, the insulator is restored. After restoring the standard electrical circuit with an SOS switch on the accelerator URT-1M the same FVI worked perfectly.

It is known that FVIs of submicrosecond accelerators [7, 8, 11] operate either with forced resistive voltage distribution between sections, or are conically shaped to use capacitive distribution [18], which provided an average strength along the dielectric surface of ~ 25 kV/cm, while the inner diameter of the dielectric was ~ 350 mm. Relatively small pulse repetition rates on these high-current accelerators did not allow the breakdown in the low-pressure gas to develop between the cone cathode holder (also performing the function of capacitive voltage distribution) and the first sections of the FVI, as found in [18].

Dosimetry results at $U_0 = 30$ kV without and after absorber (20 μm) were 19.7 kGy and 6.41 kGy (40 pulses), respectively. The calculation of the effective energy of electrons according to the method [16] gave 160 keV, which is almost half the accelerating voltage. This difference is due to the large number in the spectrum of low-energy electrons accelerating on long fronts of pulse.

4. Conclusion

It was found that in submicrosecond mode, an accelerator with a metal dielectric cathode works stably at a charging voltage of up to 35kV (accelerating ~ 350 kV). Further increase of voltage is limited by breakdown of feedthrough vacuum insulator with shielding of dielectric surface.

Acknowledgement

This work was partially funded by RFBR, Russia and Sverdlovsk region, project number 20-48-660019 p_a.

5. References

- [1] Hygiene in der Landwirtschaft durch Technologien des Fraunhofer FEP [online]; <http://www.fep.fraunhofer.de/en/Anwendungsfelder/Landwirtschaft.html>
- [2] Sokovnin S.Yu., Balezin M.E., Vazirov R.A., Timoshenkova O.R., Krivonogova A.S., Isaeva A.G., Donnik I.M., *Radiat. Phys. Chem.*, **165**, 108398, 2019; doi: 10.1016/j.radphyschem.2019.108398
- [3] Vazirov R., Sokovnin S., Romanova A., Moiseeva K., *E3S Web of Conf.*, **176**, 03016, 2020; doi: 10.1051/e3sconf/202017603016
- [4] Vazirov R.A., Sokovnin S.Yu., Krivonogova A.S., Isaeva A.G., *J. Phys.: Conf. Ser.*, **2064**, 012084, 2021; doi:10.1088/1742-6596/2064/1/012084
- [5] EUCARD2, *The ebeam power house - portfolio & concepts* [online]; https://indico.cern.ch/event/563590/contributions/2371108/attachments/1389388/2115861/G_Hommes_-_EUCARD2-_powerhouse__portfolio_ebeam_technologies.pdf

-
- [6] The Institute of Nuclear Physics of the SB RAS, *What are accelerated electrons capable of?* [online]; <https://inp.nsk.su/sites/promusk/eng/>
- [7] Remnev G., Furman E., Pushkarev A., Karpuzov S. B., Kondrat'ev N. A., Goncharov D. V., *Instrum. Exp. Tech.*, **47**, 394, 2004; doi: 10.1023/B:INET.0000032909.92515.b7
- [8] Egorov I.S., Kaikanov M.I., Lukonin E.I., Remnev G.E., Stepanov A.V., *Instrum. Exp. Tech.*, **56**(5), 568, 2013; doi: 10.1134/S0020441213050035
- [9] Sokovnin S.Yu., Balezin, M.E., *Radiat. Phys. Chem.*, **144**, 265, 2018; doi: 10.1016/j.radphyschem.2017.08.023
- [10] Sokovnin S.Yu., Balezin M.E., *Radiat. Phys. Chem.*, **196**, 110137, 2022; doi: 10.1016/j.radphyschem.2022.110137
- [11] Poloskov A., Egorov I., Nashilevskiy A., Ezhov V., Smolyanskiy E., Serebrennikov M., Remnev G., *Nucl. Instrum. Methods Phys. Res. A*, **969**, 163951, 2020; doi: 10.1016/j.nima.2020.163951
- [12] Sokovnin S.Y., Balezin M.E., Shcherbinin S.V., *Instrum Exp Tech.*, **56**, 411, 2013; doi: 10.1134/S0020441213040106
- [13] Kotov Yu.A., Rodionov N.E., Sergienko V.P., Sokovnin S.Yu., Filatov A.L., *Prib. Tekh. Eksp.*, **2**, 138, 1986.
- [14] Sokovnin S.Yu., Balezin M.E., *Vacuum*, **146**, 79, 2017; doi: 10.1016/j.vacuum.2017.09.01433
- [15] Kotov Y.A., Sokovnin S.Y., Balezin M.E., *Instrum Exp Tech.*, **46**, 379, 2003; doi: 10.1023/A:1024426724439
- [16] Sokovnin S.Yu., *Pribory i Tekhnika Eksperimenta*, **4**, 125, 1992; <https://www.scopus.com/record/display.uri?eid=2-s2.0-0026887453&origin=reflist>
- [17] Volkov S.N., Zherlitsyn A.A., Koval'chuk B.M., Loginov S.V., Pegel I.V., *Instrum Exp Tech.*, **46**(5), 656, 2003; doi: 10.1023/A:1026041705575
- [18] Egorov I., *IEEE Trans. on Dielec. and Elect.Insul.*, **23**(4), 2174, 2016; doi: 10.1109/TDEI.2016.7556492